Exploring the nonlinear dynamics of horizontal drillstrings subjected to friction and shocks effects

A. Cunha Jr, Christian Soize, R. Sampaio

EXPLORING THE NONLINEAR DYNAMICS OF HORIZONTAL DRILLSTRINGS SUBJECTED TO FRICTION AND SHOCKS EFFECTS

Americo Cunha Jr[a,b], **Christian Soize**[b] **and Rubens Sampaio**[a]

[a]*PUC–Rio, Departamento de Engenharia Mecânica*
Rua Marquês de São Vicente, 225, Gávea, Rio de Janeiro - RJ, Brasil.
americo.cunhajr@gmail.com *rsampaio@puc-rio.br*

[b]*Université Paris-Est, Laboratoire Modélisation et Simulation Multi Echelle,*
MSME UMR 8208 CNRS, 5, Boulevard Descartes 77454, Marne-la-Vallée, France.
christian.soize@univ-paris-est.fr

Keywords: nonlinear dynamics, drillstring dynamics, stick-slip, bit-bounce

Abstract. This paper presents a model to describe the nonlinear dynamics of a drillstring in horizontal configuration, which is intended to correctly predict the three-dimensional dynamics of this complex structure. This model uses a beam theory, with effects of rotatory inertia and shear deformation, which is capable of reproducing the large displacements that the beam undergoes. Also, it considers the effects of torsional friction and normal shock due to the transversal impacts between the rotating beam and the borehole wall, as well as, the force and the torque induced by the bit-rock interaction. This is done as a first effort to solve a robust optimization problem, which seeks to maximize the rate of penetration of the drillstring into the soil, to reduce the drilling process costs. Numerical simulations reported in this work shown that the developed computational model is able to quantitatively well describe the dynamical behavior of a horizontal drillstring, once its reproduces some phenomena observed in real drilling systems, such as bit-bounce, stick-slip, and transverse impacts.

1 INTRODUCTION

A drillstring is a device, used to drill oil wells, which presents an extremely complex three-dimensional nonlinear dynamics. The dynamical system associated with this physical system involves the nonlinear coupling between three different mechanisms of vibration (longitudinal, transverse, and torsional), as well as lateral and frontal shocks, due to drill-pipes/borehole and drill-bit/soil and impacts respectively (Spanos et al., 2003). Traditionally, a drillstring configuration is vertical, but directional or even horizontal configurations, where the boreholes are drilled following a non-vertical way, are also possible.

Once oil drilling a topic of great relevance in the context of engineering, the dynamics of a vertical drillstring has been studied in several works (Chevallier, 2000; Ritto et al., 2009, 2010; Chatjigeorgiou, 2013; Liu et al., 2013; Depouhon and Detournay, 2014). However, although of most of the oil wells today be drilled with columns using non-vertical configurations, very few papers in the open literature models drillstring in directional configurations (Sahebkar et al., 2011; Hu et al., 2012; Ritto et al., 2013).

Aiming to fill the gap in the scientific literature on horizontal drillstring dynamics, this work presents the modeling of a drillstring in a horizontal configuration. This model takes into account the three-dimensional dynamics of the structure, as well as the transversal/torsional effects of shock, which the structure is subject due to the impact with the borehole wall. Also, the model considers the bit-rock interaction effects, and the weight of the drilling fluid.

This rest of this paper is organized as follows. The mathematical modeling of the nonlinear dynamics appears in section 2. Then, in section 3, the results of numerical simulations are presented and discussed. Finally, in section 4, the main conclusions are emphasized and some directions for future work outlined.

2 MATHEMATICAL MODELING

2.1 Mechanical system of interest

The mechanical system of interest in this work is sketched in Figure 1. It consists of a horizontal rigid pipe (illustrated as the pair of stationary rigid walls), perpendicular to gravity acceleration g, which contains in its interior a deformable tube under rotation (rotating beam), subjected to three-dimensional displacements. This deformable tube has a length L, cross section area A, and is made of a material with mass density ρ, elastic modulus E, and Poisson ratio ν. It loses energy through a mechanism of viscous dissipation, proportional to the mass operator, with damping coefficient c. Inside the tube there is a fluid without viscosity, with mass density ρ_f. Concerning the boundary conditions, the rotating beam is blocked for transversal displacements in both extremes; blocked to transversal rotations on the left extreme; and, on the left extreme, has a constant angular velocity around x equal to Ω, and an imposed longitudinal velocity V_0.

2.2 Beam theory

The beam theory adopted takes into account the rotatory inertia and shear deformation of the beam cross section. Also, as the beam is confined within the borehole, it is reasonable to assume that it is undergoing small rotations in the transverse directions.

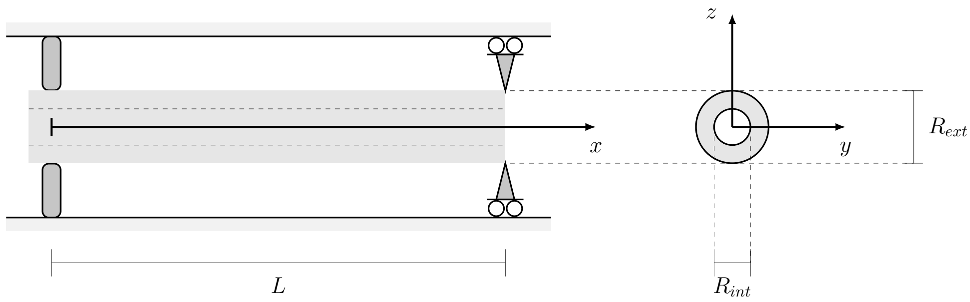

Figure 1: Schematic representation of the rotating beam which models the horizontal drillstring.

By another hand, large displacements are observed in x, y, and z. Therefore, the analysis that follows uses a beam theory which assumes large rotation in x, and large displacements the three spatial directions, which couples the longitudinal, transverse and torsional vibrations (Bonet and Wood, 2008).

Regarding the kinematic hypothesis adopted for the beam theory, it is assumed that the three-dimensional displacement of a beam point, occupying the position (x, y, z) at the instant of time t, can be written as

$$\begin{aligned} u_x(x,y,z,t) &= u - y\theta_z + z\theta_y, \\ u_y(x,y,z,t) &= v + y\,(\cos\theta_x - 1) - z\sin\theta_x, \\ u_z(x,y,z,t) &= w + z\,(\cos\theta_x - 1) + y\sin\theta_x, \end{aligned} \tag{1}$$

where letters u, v, and w are used to denote the displacements of a beam neutral fiber point in x, y, and z directions, respectively, while θ_x, θ_y, and θ_z represent rotations of the beam around the x, y, and z axes respectively. Note that these quantities depend on the position x and the time t.

2.3 Friction and shock effects

This rotating beam is also able to generate normal shocks and torsional friction in random areas of the rigid tube, which are respectively described by the Hunt and Crossley shock model Hunt and Crossley (1975), and the standard Coulomb friction model. Therefore, the force of normal shock is given by

$$F_{FS} = -k_{FS_1}\,\delta_{FS} - k_{FS_2}\,\delta_{FS}^3 - c_{FS}\,|\delta|^3\dot{\delta}_{FS}, \tag{2}$$

and the Coulomb frictional torque by

$$T_{FS} = -\mu_{FS}\,F_{FS}\,R_{bh}\,\mathtt{sgn}\left(\dot{\theta}_x\right). \tag{3}$$

In the above equations, k_{FS_1}, k_{FS_2} and c_{FS} are constants of the shock model, while μ_{FS} is a friction coefficient, R_{bh} is the borehole radius, and $\mathtt{sgn}\,(\cdot)$ the sign function. The $\dot{}$ is an abbreviation for time derivative, and the parameter $\delta_{FS} = r - \mathtt{gap}$, where $r = \sqrt{v^2 + w^2}$, is dubbed *indentation*, and is a measure of penetration in the wall of a beam cross section, such as illustrated in Figure 2.

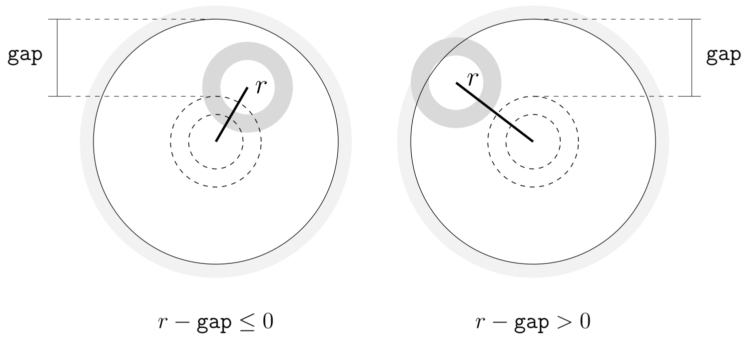

Figure 2: Illustration of the indentation parameter in a situation without impact (left) or with impact (right).

2.4 Bit-rock interaction effects

At the right extreme of the rotating beam act a force and a torque, which emulate the effects of interaction between the drill-bit and the soil. They are respectively given by

$$F_{BR} = \begin{cases} \Gamma_{BR} \left(\exp\left(-\alpha_{BR} \dot{u}(L, \cdot) \right) - 1 \right), & \text{for} \quad \dot{u}(L, \cdot) > 0 \\ 0, & \text{for} \quad \dot{u}(L, \cdot) \leq 0 \end{cases} \tag{4}$$

and

$$T_{BR} = -\mu_{BR} \, F_{BR} \, \xi_{BR} \left(\dot{\theta}_x \right), \tag{5}$$

where Γ_{BR} is the bit-rock limit force; α_{BR} is the rate of change of bit-rock force; μ_{BR} bit-rock friction coefficient; and ξ_{BR} is a regularization function, which takes into account the dimension of length, to the Eq.(5) gives a torque. The expression for the bit-rock interaction models above were, respectively, proposed by Ritto et al. (2013) and Khulief et al. (2007).

2.5 Variational formulation of the nonlinear dynamics

Using a modified version of the extended Hamilton's principle, to include the effects of dissipation, one can write the weak form of the nonlinear equation of motion of the mechanical system as

$$\mathcal{M}\left(\boldsymbol{\psi}, \ddot{\boldsymbol{U}}\right) + \mathcal{C}\left(\boldsymbol{\psi}, \dot{\boldsymbol{U}}\right) + \mathcal{K}\left(\boldsymbol{\psi}, \boldsymbol{U}\right) = \mathcal{F}_{NL}\left(\boldsymbol{\psi}, \boldsymbol{U}, \dot{\boldsymbol{U}}, \ddot{\boldsymbol{U}}\right), \tag{6}$$

where $\mathcal{M}$ represents the mass operator, $\mathcal{C}$ is the damping operator, $\mathcal{K}$ is the stiffness operator, and $\mathcal{F}_{NL}$ is the nonlinear force operator. Also, the field variables and their weight functions are lumped in the vectors fields $\boldsymbol{U} = \left(u, v, w, \theta_x, \theta_y, \theta_z\right)$, and $\boldsymbol{\psi} = \left(\psi_u, \psi_v, \psi_w, \psi_{\theta_x}, \psi_{\theta_y}, \psi_{\theta_z}\right)$.

The above operators are respectively defined by

$$
\begin{aligned}
\mathcal{M}\left(\boldsymbol{\psi},\ddot{\boldsymbol{U}}\right) \;=\; & \int_{x=0}^{L} \rho\, A \left(\psi_u\, \ddot{u} + \psi_v\, \ddot{v} + \psi_w\, \ddot{w}\right) dx \;+ \\
& \int_{x=0}^{L} \rho_f\, A_f \left(\psi_v\, \ddot{v} + \psi_w\, \ddot{w}\right) dx \;+ \\
& \int_{x=0}^{L} \rho\, I_4 \left(2\, \psi_{\theta_x}\, \ddot{\theta}_x + \psi_{\theta_y}\, \ddot{\theta}_y + \psi_{\theta_z}\, \ddot{\theta}_z\right) dx,
\end{aligned} \tag{7}
$$

$$
\begin{aligned}
\mathcal{C}\left(\boldsymbol{\psi},\dot{\boldsymbol{U}}\right) \;=\; & \int_{x=0}^{L} c\, \rho\, A \left(\psi_u\, \dot{u} + \psi_v\, \dot{v} + \psi_w\, \dot{w}\right) dx \;+ \\
& \int_{x=0}^{L} c\, \rho\, I_4 \left(2\, \psi_{\theta_x}\, \dot{\theta}_x + \psi_{\theta_y}\, \dot{\theta}_y + \psi_{\theta_z}\, \dot{\theta}_z\right) dx,
\end{aligned} \tag{8}
$$

$$
\begin{aligned}
\mathcal{K}\left(\boldsymbol{\psi},\boldsymbol{U}\right) \;=\; & \int_{x=0}^{L} E\, A\, \psi_u'\, u'\, dx \;+ \\
& \int_{x=0}^{L} E\, I_4 \left(\psi_{\theta_y}'\, \theta_y' + \psi_{\theta_z}'\, \theta_z'\right) dx \;+ \\
& \int_{x=0}^{L} 2\, \kappa_s\, G\, I_4\, \psi_{\theta_x}'\, \theta_x'\, dx \;+ \\
& \int_{x=0}^{L} \kappa_s\, G\, A \left(\left(\psi_{\theta_y} + \psi_w'\right)\left(\theta_y + w'\right) + \left(\psi_{\theta_z} - \psi_v'\right)\left(\theta_z - v'\right)\right) dx,
\end{aligned} \tag{9}
$$

and

$$
\begin{aligned}
\mathcal{F}_{NL}\left(\boldsymbol{\psi},\boldsymbol{U},\dot{\boldsymbol{U}},\ddot{\boldsymbol{U}}\right) \;=\; & \mathcal{F}_{\text{KE}}\left(\boldsymbol{\psi},\boldsymbol{U},\dot{\boldsymbol{U}},\ddot{\boldsymbol{U}}\right) + \mathcal{F}_{\text{SE}}\left(\boldsymbol{\psi},\boldsymbol{U}\right) \;+ \\
& \mathcal{F}_{\text{FS}}\left(\boldsymbol{\psi},\boldsymbol{U}\right) + \mathcal{F}_{\text{BR}}\left(\boldsymbol{\psi},\dot{\boldsymbol{U}}\right) + \mathcal{F}_{\text{G}}\left(\boldsymbol{\psi}\right),
\end{aligned} \tag{10}
$$

where

$$
\begin{aligned}
\mathcal{F}_{\text{KE}} \;=\; & -\int_{x=0}^{L} 2\, \rho\, I_4\, \psi_{\theta_x} \left(\theta_y\, \ddot{\theta}_z + \dot{\theta}_y\, \dot{\theta}_z\right) dx \\
& + \int_{x=0}^{L} 2\, \rho\, I_4\, \psi_{\theta_y} \left(\theta_y\, \dot{\theta}_z^2 + \dot{\theta}_x\, \dot{\theta}_z\right) dx \\
& - \int_{x=0}^{L} 2\, \rho\, I_4\, \psi_{\theta_z} \left(\theta_y\, \ddot{\theta}_x + \theta_y^2\, \ddot{\theta}_z\right) dx \\
& - \int_{x=0}^{L} 2\, \rho\, I_4\, \psi_{\theta_z} \left(\dot{\theta}_x\, \dot{\theta}_y + 2\, \theta_y\, \dot{\theta}_y\, \dot{\theta}_z\right) dx
\end{aligned} \tag{11}
$$

is a nonlinear force due to inertial effects;

$$
\begin{aligned}
\mathcal{F}_{\text{SE}} \;=\; & \int_{x=0}^{L} \left(\psi_{\theta_x}\,\Gamma_1 + \psi_{\theta_y}\,\Gamma_2 + \psi_{\theta_z}\,\Gamma_3\right) dx \; + \\
& \int_{x=0}^{L} \left(\psi'_u\,\Gamma_4 + \psi'_v\,\Gamma_5 + \psi'_w\,\Gamma_6\right) dx \; + \\
& \int_{x=0}^{L} \left(\psi'_{\theta_x}\Gamma_7 + \psi'_{\theta_y}\,\Gamma_8 + \psi'_{\theta_z}\,\Gamma_9\right) dx,
\end{aligned}
\tag{12}
$$

is a nonlinear force due to geometric nonlinearity;

$$
\mathcal{F}_{\text{FS}} \;=\; \sum_{m=1}^{N_{nodes}} \left(F_{\text{FS}}\left(v\,\psi_v + w\,\psi_w\right)/r + T_{\text{FS}}\,\psi_{\theta_x}\right)\Big|_{x=x_m}, \tag{13}
$$

is a nonlinear force due to the effects of friction and shock;

$$
\mathcal{F}_{\text{BR}} = F_{\text{BR}}\,\psi_u\Big|_{x=L} + T_{\text{BR}}\,\psi_{\theta_x}\Big|_{x=L}, \tag{14}
$$

is a nonlinear force due to the bit-rock interaction; and

$$
\mathcal{F}_{\text{G}} = -\int_{x=0}^{L} \left(\rho\,A + \rho_f\,A_f\right)\,g\,\psi_w\,dx, \tag{15}
$$

is a linear force due to the gravity. The nonlinear functions Γ_n, with $n = 1, \cdots, 9$, in Eq.(12) are very complex and, for sake of space limitation, are not presented here. See Cunha Jr (2015) for details.

The weak form of the initial conditions reads

$$
\mathcal{M}\left(\boldsymbol{\psi}, \boldsymbol{U}(0)\right) = \mathcal{M}\left(\boldsymbol{\psi}, \boldsymbol{U}_0\right), \tag{16}
$$

and

$$
\mathcal{M}\left(\boldsymbol{\psi}, \dot{\boldsymbol{U}}(0)\right) = \mathcal{M}\left(\boldsymbol{\psi}, \dot{\boldsymbol{U}}_0\right), \tag{17}
$$

where $\boldsymbol{U}_0$ and $\dot{\boldsymbol{U}}_0$, respectively, denote the initial displacement, and the initial velocity fields.

The model presented above is an adaptation, for the case of horizontal drillstrings, with some variations in the friction and shock treatment, of the model proposed by Ritto et al. (2009) to describe the nonlinear dynamics of vertical drillstrings.

2.6 Discretization of the model equations

The Eqs.(6), (16) and (17) are discretized by means of the standard finite element method (Hughes, 2000), using an interdependent interpolation scheme (Reddy, 1997), which adopts affine functions for the axial displacement/torsional rotation, and Hermite cubic polynomials for the transverse displacements/rotations.

Therefore, one arrives in the following initial value problem

$$[M]\,\ddot{\boldsymbol{Q}}(t) + [C]\,\dot{\boldsymbol{Q}}(t) + [K]\,\boldsymbol{Q}(t) = \boldsymbol{\mathcal{F}}\left(\boldsymbol{Q}(t), \dot{\boldsymbol{Q}}(t), \ddot{\boldsymbol{Q}}(t)\right), \tag{18}$$

and

$$[M]\,\boldsymbol{Q}(0) = \boldsymbol{Q}_0, \qquad \text{and} \qquad [M]\,\dot{\boldsymbol{Q}}(0) = \dot{\boldsymbol{Q}}_0, \tag{19}$$

where $\boldsymbol{Q}(t)$ is the nodal displacement vector (translations and rotations), $\dot{\boldsymbol{Q}}(t)$ is the nodal velocity vector, $\ddot{\boldsymbol{Q}}(t)$ is the nodal acceleration vector, $[M]$ is the mass matrix, $[C]$ is the damping matrix, $[K]$ is the stiffness matrix, and $\boldsymbol{\mathcal{F}}$ is a nonlinear force vector, which contains contributions of an inertial force and a force of geometric stiffness.

The geometric boundary conditions are included as constraints, via the method of Lagrange multipliers. Nominally, they are the velocity of translation, V_0, and the velocity of rotation, Ω, which are imposed at the left end of the beam.

2.7 Reduction of the nonlinear dynamics

To reduce the computational cost of the simulations, the initial value problem of Eqs.(18) and (19) is projected in a vector space of dimension N_{red}, spanned by the linear modes associated to the conservative part of the underlying linear dynamical system. This results in the reduced initial value problem given by

$$[M]\,\ddot{\boldsymbol{q}}(t) + [C]\,\dot{\boldsymbol{q}}(t) + [K]\,\boldsymbol{q}(t) = \boldsymbol{f}\left(\boldsymbol{q}(t), \dot{\boldsymbol{q}}(t), \ddot{\boldsymbol{q}}(t)\right), \tag{20}$$

and

$$\boldsymbol{q}(0) = \boldsymbol{q}_0, \qquad \text{and} \qquad \dot{\boldsymbol{q}}(0) = \dot{\boldsymbol{q}}_0, \tag{21}$$

which is integrated using the Newmark method (Newmark, 1959), and the nonlinear system of algebraic equations, resulting from the time discretization, is solved by a fixed point iteration.

3 RESULTS AND DISCUSSION

In order to simulate the nonlinear dynamics of the mechanical system, the physical parameters presented in the Table 1 are adopted, as well as the length $L = 35\ m$, the rotational and axial velocities in x, respectively given by $\Omega = 2\pi\ rad/s$, and $V_0 = 1/720\ m/s$. For the geometry discretization, 105 finite elements are used. This results in FEM model with 636 degrees of freedom. In the reduced order model, 51 DOF are considered.

The dynamics is investigated for a "temporal window" of $90s$, with a nominal time step $\Delta t = 69\ ms$, which is refined whenever necessary to capture the effects of shock. For the initial conditions, the static equilibrium configuration of the beam is adopted.

The drill-bit longitudinal displacement and velocity, can be seen in Figure 3. It is noted that, during the interval of analysis, the column presents an advance in the forward direction with small axial oscillations. These axial oscillations, which are more pronounced in the velocity curve, correspond to the vibration mechanism known as *bit-bounce*, where the drill-bit loses contact with the soil and then hits the rock abruptly. This phenomenon is widely observed in real systems (Spanos et al., 2003).

Table 1: Physical parameters of the mechanical system that are used in the simulation.

parameter	value	unit
ρ	7900	kg/m^3
ρ_f	1200	kg/m^3
E	203	GPa
ν	0.3	—
R_{int}	40	mm
R_{ext}	60	mm
R_{bh}	70	mm
c	0.03	—
g	9.81	m/s^2
k_{FS_1}	1×10^{10}	N/m
k_{FS_2}	1×10^{16}	N/m^3
c_{FS}	$1 \times 10^{\ 9}$	$(N/m^3)/(m/s)$
μ_{FS}	1×10^{-5}	—
Γ_{BR}	250	kN
α_{BR}	180	$1/(m/s)$
μ_{BR}	400×10^{-4}	—

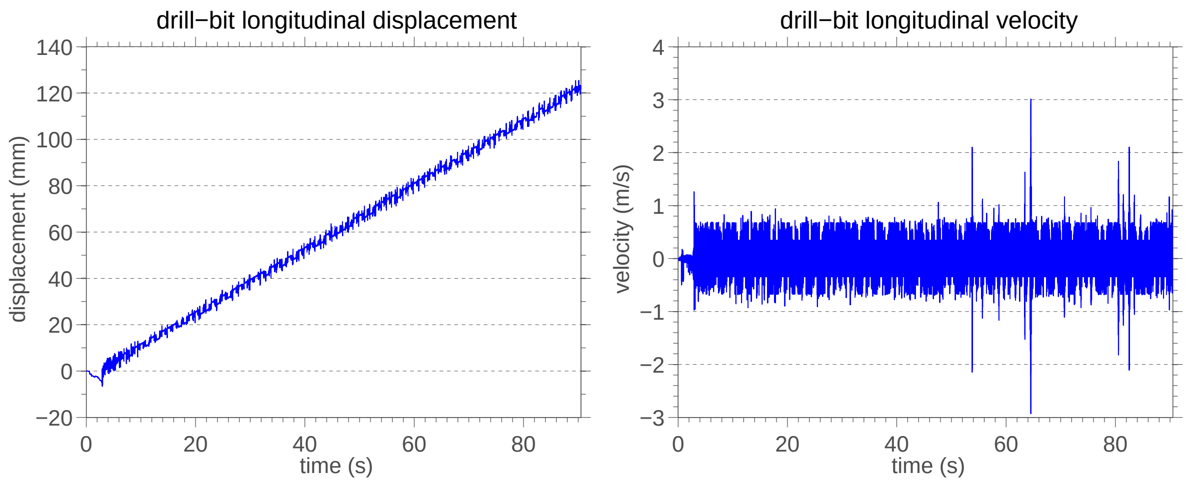

Figure 3: Illustration of the drill-bit displacement (left) and of the drill-bit velocity (right).

The drill-bit rotation and angular velocity, can be seen in Figure 4. What it is observed now is a almost monotonic rotation. However, when one looks to the angular velocity, it is possible to see packages of fluctuations with amplitude variations that can reach up to four orders of magnitude. This indicates that the drill-bit undergoes a blockage due to the torsional friction, and then it is released subtly, so that its velocity is sharply increased, in a *stick-slip* phenomenon type. This is also seen experimentally (Spanos et al., 2003) in real drilling systems.

The evolution of the radial displacement, for $x = 20$, of the beam cross-section can be seen in the Figure 5. Analyzing this figure it is clear that transverse impacts between the drillstring and the borehole wall occur during the drilling process, which is also reported experimentally (Spanos et al., 2003).

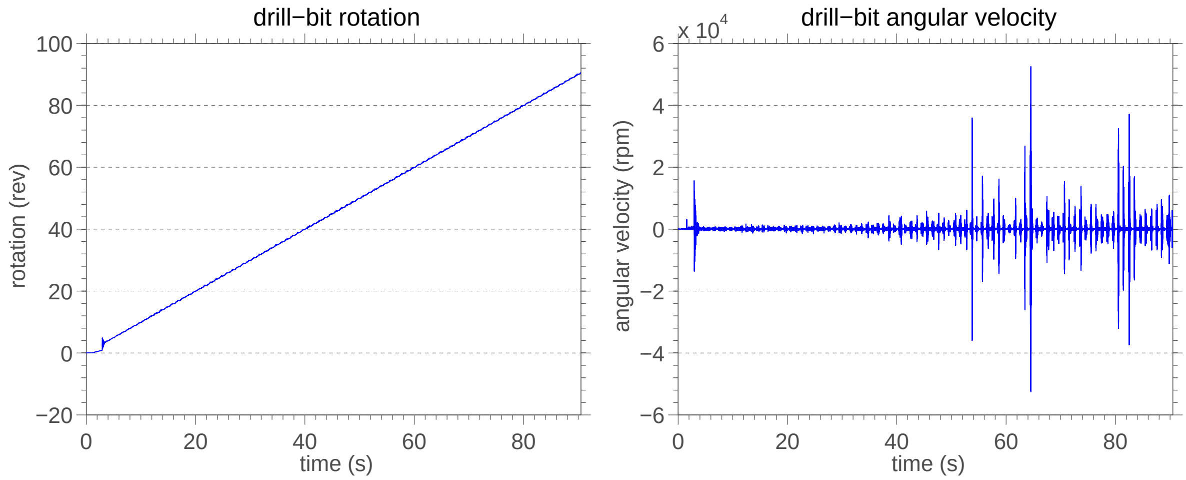

Figure 4: Illustration of the drill-bit rotation (left) and of the drill-bit angular velocity (right).

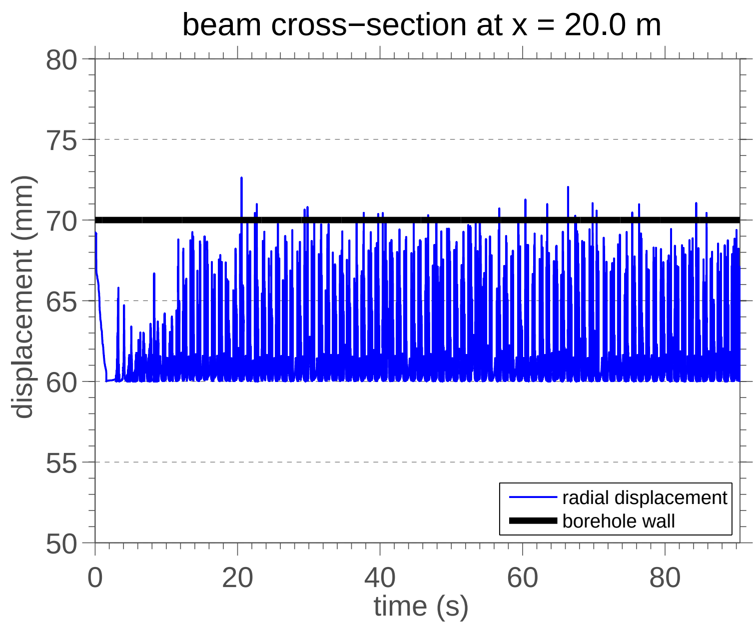

Figure 5: Illustration of the beam radial displacement for $x = 20\ m$.

4 CONCLUDING REMARKS

A model was developed in this work to describe the nonlinear dynamics of horizontal drillstrings. The model uses a beam theory, with effects of rotatory inertia and shear deformation, which is capable of reproducing the large displacements that the beam undergoes. This model also considers the effects of friction and shock due to the transversal impacts between the beam and the borehole wall, as well as, the force and the torque induced by the bit-rock interaction.

Numerical simulations reported in this work shown that the developed computational model is able to quantitatively well describe the dynamical behavior of a horizontal drillstring, once its reproduces some phenomena observed in real drilling systems, such as bit-bounce, stick-slip, and transverse impacts.

In a future work, the authors intend to develop a stochastic modeling of the nonlinear dynamics of horizontal drillstrings, in order to quantify the uncertainties associated with this problem, which are due to the variability of its parameters (Schuëller, 2007), and/or epistemic in nature, i.e., result of the ignorance about the physics of the problem (Soize, 2013). Also, in a next step, they want to solve an robust optimization problem, which seeks to maximize the rate of penetration of the column into the soil (Ritto et al., 2010).

ACKNOWLEDGMENTS

The authors are indebted to the Brazilian agencies CNPq, CAPES, and FAPERJ, and the French agency COFECUB for the financial support given to this research. They would also like to acknowledge professors Anas Batou and Thiago Ritto for valuable discussions on this work.

REFERENCES

Bonet J. and Wood R.D. *Nonlinear Continuum Mechanics for Finite Element Analysis*. Cambridge University Press, Cambridge, 2nd edition, 2008.

Chatjigeorgiou I.K. Numerical simulation of the chaotic lateral vibrations of long rotating beams. *Applied Mathematics and Computation*, 219:5592–5612, 2013. doi:10.1016/j.amc.2012.11.076.

Chevallier A. *Nonlinear Stochastic Drilling Vibrations*. Ph.D Thesis, Rice University, Houston, 2000.

Cunha Jr A. *Modeling and Uncertainty Quantification in the Nonlinear Stochastic Dynamics of a Horizontal Dsrillstrings*. D.Sc. Thesis, Pontifícia Universidade Católica do Rio de Janeiro / Université Paris-Est, 2015.

Depouhon A. and Detournay E. Instability regimes and self-excited vibrations in deep drilling systems. *Journal of Sound and Vibration*, 333:2019–2039, 2014. doi:10.1016/j.jsv.2013.10.005.

Hu Y., Di Q., Zhu W., Chen Z., and Wang W. Dynamic characteristics analysis of drillstring in the ultra-deep well with spatial curved beam finite element. *Journal of Petroleum Science and Engineering*, 82—83:166–173, 2012. doi:10.1016/j.petrol.2012.01.011.

Hughes T.J.R. *The Finite Element Method*. Dover Publications, New York, 2000.

Hunt K.H. and Crossley F.E. Coefficient of restitution interpreted as damping in vibroimpact. *Journal of Applied Mechanics*, 42:440–445, 1975. doi:10.1115/1.3423596.

Khulief Y.A., Al-Sulaiman F.A., and Bashmal S. Vibration analysis of drillstrings with self-excited stick–slip oscillations. *Journal of Sound and Vibration*, 299:540–558, 2007. doi:10.1016/j.jsv.2006.06.065.

Liu X., Vlajic N., Long X., Meng G., and Balachandran B. Nonlinear motions of a flexible rotor with a drill bit: stick-slip and delay effects. *Nonlinear Dynamics*, 72:61–77, 2013. doi:10.1007/s11071-012-0690-x.

Newmark N.M. A method of computation for structural dynamics. *Journal of the Engineering Mechanics Division*, 85:67–94, 1959.

Reddy J.N. On locking-free shear deformable beam finite elements. *Computer Methods in Applied Mechanics and Engineering*, 149:113–132, 1997. doi:10.1016/S0045-7825(97)00075-3.

Ritto T.G., Escalante M.R., Sampaio R., and Rosales M.B. Drill-string horizontal dynamics with uncertainty on the frictional force. *Journal of Sound and Vibration*, 332:145–153, 2013. doi:10.1016/j.jsv.2012.08.007.

Ritto T.G., Soize C., and Sampaio R. Non-linear dynamics of a drill-string with uncertain model of the bit–rock interaction. *International Journal of Non-Linear Mechanics*, 44:865–876, 2009. doi:10.1016/j.ijnonlinmec.2009.06.003.

Ritto T.G., Soize C., and Sampaio R. Robust optimization of the rate of penetration of a drill-string using a stochastic nonlinear dynamical model. *Computational Mechanics*, 45:415–427, 2010. doi:10.1007/s00466-009-0462-8.

Sahebkar S.M., Ghazavi M.R., Khadem S.E., and Ghayesh M.H. Nonlinear vibration analysis of an axially moving drillstring system with time dependent axial load and axial velocity in inclined well. *Mechanism and Machine Theory*, 46:743–760, 2011. doi:10.1016/j.mechmachtheory.2010.12.003.

Schuëller G.I. On the treatment of uncertainties in structural mechanics and analysis. *Computers & Structures*, 85:235–243, 2007. doi:10.1016/j.compstruc.2006.10.009.

Soize C. Stochastic modeling of uncertainties in computational structural dynamics — recent theoretical advances. *Journal of Sound and Vibration*, 332:2379—2395, 2013. doi:10.1016/j.jsv.2011.10.010.

Spanos P.D., Chevallier A.M., Politis N.P., and Payne M.L. Oil and gas well drilling: a vibrations perspective. *The Shock and Vibration Digest*, 35:85–103, 2003.